JVSTB Journal of Vacuum Science & Technology B

Growth and structural characteristics of Ga N Al N /nanothick - Al 2 O 3 Si (111)

W. C. Lee, Y. J. Lee, L. T. Tung, S. Y. Wu, C. H. Lee, M. Hong, H. M. Ng, J. Kwo, and C. H. Hsu

Citation: Journal of Vacuum Science & Technology B **26**, 1064 (2008); doi: 10.1116/1.2905241
View online: http://dx.doi.org/10.1116/1.2905241
View Table of Contents: http://scitation.aip.org/content/avs/journal/jvstb/26/3?ver=pdfcov
Published by the AVS: Science & Technology of Materials, Interfaces, and Processing

Growth and structural characteristics of GaN/AlN/nanothick γ-Al_2O_3/Si (111)

W. C. Lee, Y. J. Lee, L. T. Tung, S. Y. Wu, C. H. Lee, and M. Hong[a),b)]
Department of Materials Science and Engineering, National Tsing Hua University, HsinChu 30013, Taiwan

H. M. Ng
Bell Labs, Alcatel-Lucent, Murray Hill, New Jersey 07974

J. Kwo[a),c)]
Department of Physics, National Tsing Hua University, Hsinchu 30013, Taiwan

C. H. Hsu[d)]
Research Division, National Synchrotron Radiation Research Center, Hsinchu 30013, Taiwan

(Received 26 October 2007; accepted 10 March 2008; published 30 May 2008)

The authors report on the growth of GaN by nitrogen plasma-assisted molecular beam epitaxy (MBE) on a 2 in. Si (111) substrates with a nanothick (~4.8 nm thick) γ-Al_2O_3 as a template/buffer. A thin layer of MBE-AlN ~40 nm thick was inserted prior to the growth of GaN. High-resolution transmission electron microscopy (HR-TEM) and high-resolution x-ray diffraction studies indicated that both of the nanothick γ-Al_2O_3 and AlN are a single crystal. Reflection high-energy electron diffraction, high-resolution x-ray scattering using synchrotron radiation, and cross-sectional HR-TEM measurements indicated an orientation relationship of $GaN(0002)\|AlN(0002)\|\gamma\text{-}Al_2O_3(111)\|Si(111)$ and $GaN[10-10]\|AlN[10-10]\|\gamma\text{-}Al_2O_3[2-1-1]\|Si[2-1-1]$. A dislocation density of $5\times(10^8-10^9)/cm^2$ in the GaN ~0.5 μm thick was determined using cross-sectional TEM images under weak-beam dark-field conditions.
 [DOI: 10.1116/1.2905241]

I. INTRODUCTION

III-nitride compound semiconductors, besides being essential for producing blue lasers and light emitting diodes, are suitable for applications in high-temperature and high-power electronics because of their wide band gaps and high breakdown fields. The epitaxial growth of GaN on silicon offers several advantages over that on sapphire or SiC, including substrates with high crystal quality, cost advantages, and integration of high-power electronics and/or optoelectronics with the most advanced Si-based integrated circuits. Direct growth of GaN on Si, however, is extremely difficult due to a large lattice mismatch of ~17% [$a_{GaN(0001)}$ =3.189 Å and $a_{Si(111)}$=3.840 Å] and difference in thermal expansion coefficients of ~33% between GaN and Si. Single crystal GaN has been successfully grown on nanothick oxides such as single crystal Gd_2O_3,[1] which has also been deposited on Si (111) with good crystalline quality.[2,3] In addition, numerous intermediate layers, including AlN,[4,5] HfN,[6] SiN,[7] and Al_2O_3,[8] have been employed to effectively facilitate epitaxial growth of GaN on Si. Recently, nanothick cubic γ-Al_2O_3 single crystal films epitaxially grown on Si (111) with high crystal quality have been obtained using electron beam evaporation under ultrahigh vacuum.[9] Cubic γ-Al_2O_3 has a defective Spinel structure which is different from the more common corundum structure of α-Al_2O_3 (sapphire). Nevertheless, the in-plane symmetry of the γ-Al_2O_3 films is similar to that of sapphire (0001) (α-Al_2O_3), which has been commonly used for GaN growth.

In this work, we have succeeded in achieving epitaxial growth of GaN using nitrogen plasma-assisted molecular beam epitaxy (MBE) on the γ-Al_2O_3/Si (111). *In situ* reflection high-energy electron diffraction (RHEED) has exhibited the initial growth of GaN (AlN), showing streaky patterns with a bright intensity, indicating an epitaxial growth right at the beginning. The epitaxial interfacial characteristics among GaN/AlN/γ-Al_2O_3/Si and the crystal defects including dislocations in GaN have been studied using high-resolution transmission electron microscopy (HR-TEM) and high-resolution x-ray diffraction using synchrotron radiation source. The chemical information on the heterostructure, particularly at the interface, performed using energy-filtering transmission electron microscope (EF-TEM), has indicated that no Si diffusion through the γ-Al_2O_3 into GaN (AlN).

II. EXPERIMENT

The cleaning and hydrogen passivation of Si (111) wafers were performed with an RCA method and a HF dip prior to being placed into an oxide chamber in a multichamber MBE system.[10] The Si surface was further cleaned with heating the wafers to temperatures above ~700 °C, resulting in a sharp, streaky (7×7) reconstructed RHEED pattern with Kikuchi arcs, indicative of the attainment of a clean surface of Si (111) substrate.[11] The thin γ-Al_2O_3 films were then deposited on the reconstructed Si surface with electron beam evapora-

a)Author to whom correspondence should be addressed.
b)Electronic mail: mhong@mx.nthu.edu.tw
c)Electronic mail: raynien@phys.nthu.edu.tw
d)Also at Department of Photonics, National Chiao Tung University, Hsinchu, Taiwan.

tion from a high-purity sapphire target. During the oxide deposition, the vacuum in the chamber was maintained in the low 10^{-8} torr (even with the evaporation of sapphire) and substrate temperatures were maintained at about 720–780 °C. Streaky oxide RHEED patterns along the in-plane axes of [1−10] and [11−2] of Si were observed after growth of oxide 1 nm thick. This indicates that a smooth crystalline γ-Al_2O_3 film formed on the Si (111), with an in-plane alignment between the oxide film and Si substrate.

The samples of γ-Al_2O_3/Si were then transferred *ex situ* to another MBE system for the GaN epilayer growth. The samples were outgassed in the preparation chamber before loading to the growth chamber. The substrates were exposed to nitrogen plasma to nitridate the surface. Group III elements (Ga, Al) and Si (*n*-type dopant) were evaporated using standard effusion cells. The substrate temperatures for growing GaN were at ~580 °C in the beginning and at 720 °C for the rest of the growth. The detailed GaN growth was previously published.[12] The GaN had a streaky (2×2) RHEED pattern at the end of growth.

HR-TEM specimens were prepared with mechanical polishing, dimpling, and ion milling using a Gatan PIPS system operated at 4 keV. HR-TEM was performed on a field-emission microscopy (Tecnai G^2) operated at 200 kV.

The x-ray scattering experiments were performed at wiggler beamline BL17B1 at the National Synchrotron Radiation Research Center (NSRRC), Hsinchu, Taiwan. The incident x-rays were vertically focused with a mirror and monochromatisized to 10 keV energy by a Si (111) double crystal monochromator. The sagital bending of the second crystal focused the x-rays in the horizontal direction. The dimensions of beam size are about 2×0.2 mm^2 ($H\times V$) at the sample position. With two pairs of slits between sample and detector, typical wave-vector resolution in the vertical scattering plane was set at ~0.01 nm^{-1}. High-resolution single crystal x-ray scattering measurements were carried out in the single crystal geometry.

III. RESULTS AND DISCUSSION

An AlN buffer layer was initially nucleated on the thin γ-Al_2O_3 template, followed by the growth of GaN films. Judging from the RHEED streak spacing, with the largest for Al_2O_3, followed by AlN and GaN, the in-plane lattice constants are $a_{GaN}>a_{AlN}>a_{Al2O3}$. The benefit of our work is that the growth of nitrides on γ-Al_2O_3 coated Si (111) has placed the nitride films in a compressive strain, which helps prevent cracking from occurring. If nitrides are directly grown on Si (111), GaN tends to crack after a certain thickness due to tensile strain.

Figure 1 shows a sequence of real-time RHEED images taken at different stages of the growth. Figure 1(a) reveals the high-quality γ-Al_2O_3 film grown on Si (111).[8] The sample was outgassed in the preparation chamber without any other cleaning after being transferred *ex situ* from the oxide chamber of the multichamber MBE system. Followed by the growth of AlN and GaN epilayers, as shown from the RHEED images, a sequence of line scans was taken from the

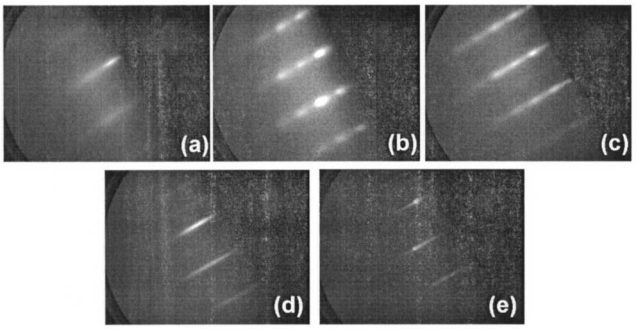

FIG. 1. Real-time RHEED of different stages. (a) γ-Al_2O_3 at low temperatures (~200 °C). (b) 10 min of AlN growth (~40 nm). (c) 5 min of GaN growth (~11 nm). (d) 45 min of GaN growth (~100 nm). (e) 4 h of GaN growth (~0.5 μm). The streakiness of the GaN pattern improves as a function of time.

RHEED images; cross sections of the streak pattern taken perpendicular to the RHEED streaks indicate that the AlN relaxes due to the lattice mismatch. When GaN was deposited on the AlN, initially, it was strained and then relaxed as the thickness increased. Also, the full width at half maximum (FWHM) of the streaks decreases as the growth proceeds. Therefore, the "streakiness" of the GaN pattern improved as a function of time. At the end of the GaN growth, a (2×2) reconstruction RHEED pattern was observed, indicating a Ga polarity surface.

A high-resolution x-ray diffraction scan along GaN/AlN/γ-Al_2O_3/Si(111) normal is shown in Fig. 2, where the abscissa is in the unit of reciprocal lattice (rlu) of GaN. From the position and intensity of the diffraction peaks, the wurzite GaN (0002), AlN (0002), and γ-Al_2O_3 (222) peaks were clearly defined. An extra peak centered at 2.21 rlu appears in some samples and its origin are still under investigation. The FWHM of the theta-rocking scan is $0.45\pm0.005°$ (exhibited in the inset) which was carried out at the GaN (0002) peak position. This means that the GaN

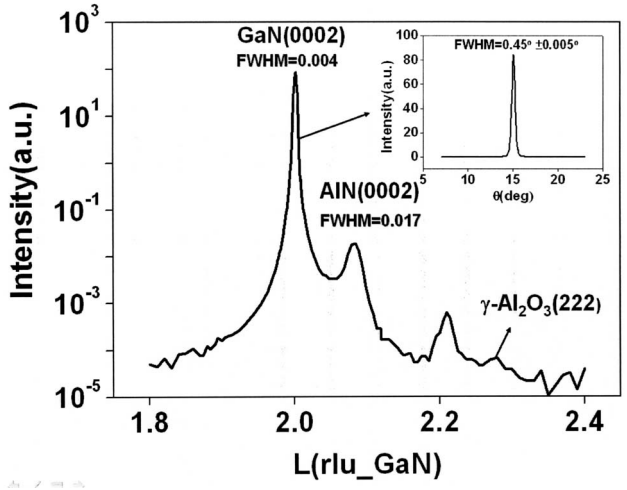

FIG. 2. Radial scan along surface normal of a GaN/AlN/γ-Al_2O_3/Si(111) sample. The theta-rocking curve of GaN (0002) reflection is illustrated in the inset.

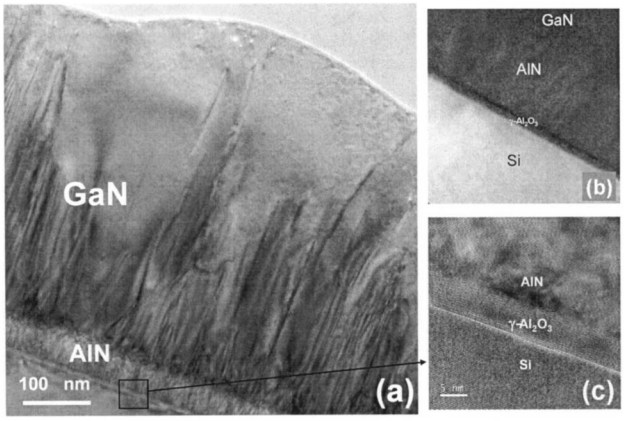

FIG. 3. (a) Cross-sectional micrograph of GaN ($\sim$0.5 μm)/AlN (41.6 nm)/γ-Al_2O_3 (4.8 nm)/Si(111) heterostructure, (b) Si $L_{2,3}$ edge energy-filtering transmission electron microscope (EF-TEM) mapping, and (c) high-magnification image of γ-Al_2O_3 (4.8 nm)/Si(111) interface.

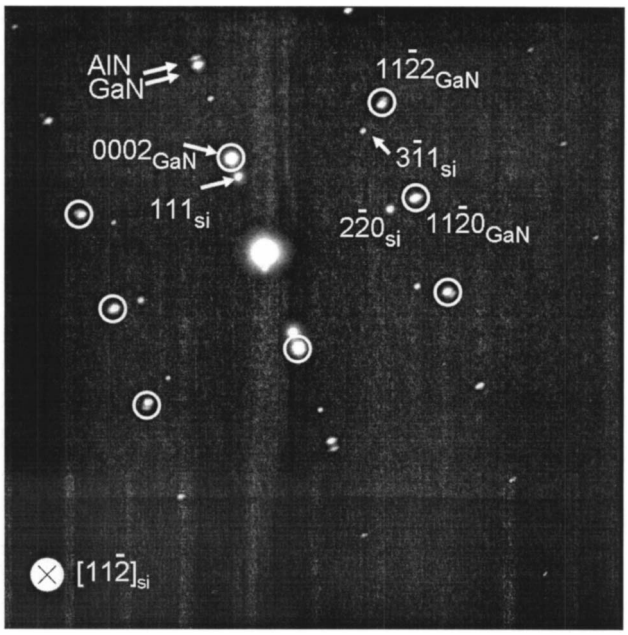

FIG. 4. Selected area diffraction pattern (SADP) of the sample discussed in Figs. 2 and 3. The incident electron beam was directed perpendicular to the (11−2) plane of Si.

film grown on top of AlN/γ-Al_2O_3 buffer has good crystalline quality, especially for a GaN $\sim$0.5 μm thick. This thickness is too thin to develop a well GaN structure, thus, expecting to contain a lot of defects such as dislocations. The FWHM of the theta-rocking curve would be smaller if a thicker GaN film were grown.

From the phi-cone scan, the symmetry and alignment of the films and substrate were determined. The orientation relationships between the nitride films, the oxide buffer, and Si substrate were given: GaN(0002)$\|$AlN(0002)$\|$$\gamma$-$Al_2O_3(111)\|$Si(111) from the normal-plane theta-two theta scan and the in-plane orientation of GaN[10−10]$\|$AlN[10−10]$\|$$\gamma$-$Al_2O_3$[2−1−1]$\|$Si[2−1−1] from the phi-cone scan of the out-of-plane Bragg peaks.

TEM studies on the heterostructure of GaN/AlN/γ-Al_2O_3/Si (111) were performed with a cross-sectional micrograph shown in Fig. 3, with (a) showing the low-magnification image and displaying the thickness of GaN, AlN, and γ-Al_2O_3 film to be $\sim$0.5 μm, 41.6 nm, and 4.8 nm, respectively. Owing to the lattice mismatch of GaN, AlN, and γ-Al_2O_3, a high density of dislocations were obviously present in the GaN and AlN films. The γ-Al_2O_3 template/buffer epilayer is further illustrated in Fig. 3(c). A clear transition was observed from Si to the epitaxial γ-Al_2O_3 film. Both γ-Al_2O_3 and its interface with Si have remained intact, as observed from TEM (namely, an atomically smooth oxide/Si interface), even they have been subjected to very severe conditions, such as the nitride growth temperatures of $\sim$750 °C and nitrogen plasma bombardments. Furthermore, the AlN/γ-Al_2O_3 interface remained relatively sharp and smooth, again indicating the robustness of γ-Al_2O_3 4.8 nm thick.

It is commonly observed that Si diffuses into GaN during the MBE growth, even for a substrate temperature of 660 °C.[13] We, therefore, performed an EF-TEM mapping to investigate the Si distribution in our sample. EF-TEM is a powerful tool for the quick composition analysis of materials, which is able to two dimensionally map specific elements. Figure 3(b) shows the EF-TEM image acquired from silicon $L_{2,3}$ edge using the standard three-window method (two pre-edge and postedge), which displays the spatial distribution of the element within the analyzed specimen area. The brighter contrast means a higher Si concentration. It reveals that the interdiffusion of Si into GaN (AlN) was blocked by the γ-Al_2O_3 buffer layer. Hence, the nanothick single crystal γ-Al_2O_3 template not only has provided as a nucleation layer for GaN (AlN) but also has prevented interdiffusion of Si at the interface. The elimination of Si interdiffusion has avoided the high unintentional doping levels in the GaN films, critical for device performance.

Figure 4 shows a corresponding selected area diffraction pattern (SADP) of the GaN/AlN/γ-Al_2O_3/Si(111) heterostructures [Fig. 3(a)] along the [11−2] zone of Si substrate. The indexed diffracted spots of GaN film and Si substrate indicate the orientation relationship between the grown GaN film and Si substrate. It appears that the GaN/Si(111) sample exhibits an orientation relationship of GaN (0001) in parallel with Si (111). The GaN (11−20) planes of GaN film were also observed to be parallel to the (1−10) planes of Si substrate.

In order to identify a dislocation density in GaN film, cross-sectional TEM images under weak-beam dark-field conditions were taken, as shown in Fig. 5. According to a basic theory for characterizing Burgers vectors with TEM observations, the dislocation is shown out of contrast when $g \cdot b = 0$. On the basis of this $g \cdot b = 0$ criterion, cross-sectional TEM images under weak-beam dark-field conditions of Fig. 5(a) g [11−20] and Fig. 5(b) g [11−22] were investigated. The dislocation density is calculated by counting along a

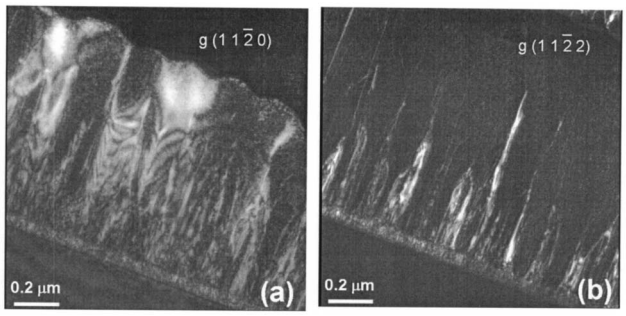

FIG. 5. TEM images under weak-beam dark-field conditions of (a) $g=(11-20)$ and (b) $g=(11-22)$ on the sample discussed in Figs. 2 and 3.

plane normal to the growth direction. Several measurements have been made in this manner at various positions across the whole film. A dislocation density in the range of $5\times(10^8-10^9)/\mathrm{cm}^2$ was then concluded.

IV. CONCLUSION

In summary, we have grown GaN on 2 in. Si (111) substrates by nitrogen plasma-assisted molecular beam epitaxy with a thin single crystal layer of γ-Al_2O_3 as the buffer layer. The γ-Al_2O_3 template provides not only a compressive strained nucleated layer for GaN but also prevents interdiffusion of Si at the interface. The GaN film with the thickness about 0.5 μm grown on γ-Al_2O_3 exhibits a good crystal quality and the dislocation density is around $5\times(10^8-10^9)/\mathrm{cm}^2$. An orientation relationship of $\mathrm{GaN}(0002)\|\mathrm{AlN}(0002)\|\gamma\text{-}\mathrm{Al_2O_3}(111)\|\mathrm{Si}(111)$ and $\mathrm{GaN}[10-10]\|\mathrm{AlN}[10-10]\|\gamma\text{-}\mathrm{Al_2O_3}[2-1-1]\|\mathrm{Si}[2-1-1]$ was determined by RHEED, high-resolution x-ray diffraction, and high-resolution transmission electron microscopy.

ACKNOWLEDGMENT

The authors wish to thank the National Science Council, Taiwan for supporting this work. We would also like to acknowledge the support from the Asian Office of Aerospace Research and Development of the U.S. Air Force.

[1] M. Hong, A. R. Kortan, H. M. Ng, J. Kwo, S. N. G. Chu, J. P. Mannaerts, A. Y. Cho, C. M. Lee, J. I. Chyi, and K. A. Anselm, J. Vac. Sci. Technol. B **20**, 1274 (2002).
[2] T. D. Lin, M. C. Hang, C. H. Hsu, J. Kwo, and M. Hong, J. Cryst. Growth **301/302**, 386 (2007).
[3] A. Fissel, D. Kühne, E. Bugiel, and H. J. Osten, Appl. Phys. Lett. **88**, 153105 (2006).
[4] S. Raghavan, X. Weng, E. Dickey, and J. M. Redwing, Appl. Phys. Lett. **87**, 142101 (2005).
[5] B. H. Bairamov, O. Gürdal, A. Botchkarev, H. Morkoç, G. Irmer, and J. Monecke, Phys. Rev. B **60**, 16741 (1999).
[6] R. Armitage, Q. Yang, H. Feick, J. Gebauer, E. R. Weber, S. Shinkai, and K. Sasaki, Appl. Phys. Lett. **81**, 1450 (2002).
[7] K. J. Lee, E. H. Shin, and K. Y. Lim, Appl. Phys. Lett. **85**, 1502 (2004).
[8] L. Wang, X. Liu, Y. Zan, J. Wang, D. Wang, D. C. Lu, and Z. Wang, Appl. Phys. Lett. **72**, 109 (1998).
[9] S. Y. Wu, M. Hong, A. R. Kortan, J. Kwo, J. P. Mannaerts, W. C. Lee, and Y. L. Huang, Appl. Phys. Lett. **87**, 091908 (2005).
[10] M. Hong, J. P. Mannaerts, J. E. Bowers, J. Kwo, M. Passlack, W.-Y. Hwang, and L. W. Tu, J. Cryst. Growth **175/176**, 422 (1997).
[11] M. Hong, A. R. Kortan, P. Chang, Y. L. Huang, C. P. Chen, H. Y. Chou, H. Y. Lee, J. Kwo, M.-W. Chu, C. H. Chen, L. V. Goncharova, E. Garfunkel, and T. Gustafsson, Appl. Phys. Lett. **87**, 251902 (2005).
[12] H. M. Ng, T. D. Moustakas, and S. N. G. Chu, Appl. Phys. Lett. **76**, 2818 (2000).
[13] E. Calleja, M. A. Sanchez-Garcia, D. Basak, F. J. Sanchez, F. Calle, P. Youinou, E. Munoz, J. J. Serrano, J. M. Blanco, C. Villar, T. Laine, J. Oila, K. Saarinen, P. Hautojärvi, C. H. Molloy, D. J. Somerford, and I. Harrison, Phys. Rev. B **58**, 1550 (1998).